International Journal of Thermal Sciences 117 (2017) 316–327

Contents lists available at ScienceDirect

International Journal of Thermal Sciences

journal homepage: www.elsevier.com/locate/ijts

Modelling steady-state thermal behaviour of double thermal network pipes

Bram van der Heijde [a, b, c, *], Arnout Aertgeerts [a, b, 1], Lieve Helsen [a, b]

[a] EnergyVille, Thor Park, Poort Genk 8310, 3600 Genk, Belgium
[b] KU Leuven, Department of Mechanical Engineering, Celestijnenlaan 300 Box 2421, 3001 Leuven, Belgium
[c] VITO, Boeretang 200, 2400 Mol, Belgium

ARTICLE INFO

Article history:
Received 9 December 2016
Received in revised form
17 March 2017
Accepted 27 March 2017

Keywords:
Heat losses
Thermal network
District heating
Linearization
Analytical model
Double pipes

ABSTRACT

Optimal design and operation of district heating networks require accurate, but simple models to allow fast simulation. This paper describes the analytical derivation of such a model based on existing work regarding heat loss and dynamic temperature profile calculations in literature. The most important addition from this work is the incorporation and investigation of heat transfer from supply to return side in double pipes, something which is often (over)simplified in more commonly used models.

The paper presents the mathematical derivations and the assumptions made in detail for the case of steady-state heat losses in double pipes. The resulting model is carefully examined in a parameter study, from which a number of interesting conclusions can be drawn. Firstly, the heat losses are found to be nearly independent of the mass flow rate in the range of mass flow rates usually encountered in thermal network pipes. The remaining heat loss calculation is simply based on temperature levels and thermal resistance factors, determined by the pipe dimensions and materials. Furthermore, it is found that heat losses from supply to return side should be incorporated in the analysis for better accuracy of the results, even more so with the increasing popularity of twin pipes with common insulation.

1. Introduction

Fourth generation district heating and cooling networks are considered as an important technology in the effort towards a more sustainable and renewable energy system [1]. The installation of these systems has been deemed beneficial both by academia and government, see for instance the Heat Roadmap Europe 2050 [2,3] and the EU Strategy on Heating and Cooling [4,5]. The latter identifies the potential of supplying 50% of the EU heat demand with district heating. These systems are characterized by lower and fluctuating supply temperatures in order to enable the inclusion of renewable energy systems, waste heat and higher efficiency heating and cooling systems. Overall, the complexity of the thermal network increases, which calls for detailed pre-studies for design and high-performing simulation models towards improved control strategies.

The study of heat losses in buried pipes is an important subject within the research towards the operation and optimization of thermal networks. As may be seen from the literature study below, many approaches towards the calculation of the behaviour of buried pipes have been proposed already, all depending on the available computation techniques and purpose of the model. This paper aims at determining the degree of mutual influence of double district heating pipes buried underground, and at accurately calculating the outlet temperatures and heat losses. Therefore, an analytical solution to the steady-state thermal problem of buried pipes is proposed, based on existing techniques for heat loss and temperature propagation calculation in these systems.

The outline of the paper is as follows: firstly, an overview of existing literature is presented, summarizing the relevant research that has inspired this new calculation technique. In the Methodology section, the mathematical derivation of the newly proposed solution is written out. The Result section presents a study regarding the sensitivity of different parameters in the model, the outcome of which is analysed and synthesized further in the Discussion and Conclusion sections.

* Corresponding author. EnergyVille, Thor Park, Poort Genk 8310, 3600 Genk, Belgium.
E-mail address: Bram.vanderHeijde@energyville.be (B. van der Heijde).
[1] Present affiliation: Actility, Sinter-Goedeleplein 5, 1000 Brussels, Belgium.

http://dx.doi.org/10.1016/j.ijthermalsci.2017.03.026

Nomenclature

Subscripts

$\square_a$	Asymmetrical problem
$\square_s$	Symmetrical problem
$\square_r$	Return *(Rücklauf)*
$\square_v$	Supply *(Vorlauf)*
$\square_{in}$	Inlet
$\square_{out}$	Outlet
$\square_b$	Boundary/Undisturbed ground

Symbols

A	Area (m^2)
C	Heat capacity per meter (J/(m K))
c_p	Specific heat capacity (J/(kg K))
f_D	Darcy friction coefficient (−)
h	Shape factor (−)
k	Thermal conductivity (W/(m K))
L	Length of the pipes (m)
p	Pressure (Pa)
$\dot{q}$	Heat flow rate per meter (W/m)
$\dot{Q}$	Heat flow rate (W)
R	Thermal resistance per meter (Km/W)
S	Circumference (m)
T	Temperature (° C)
u	Specific internal energy (J/kg)
v	Velocity (m/s)
ξ_L	Temperature decay factor (−)
ρ	Mass density (kg/m^3)
τ	Time constant (s)
ϑ	Temperature ratio (−)

2. Previous studies

2.1. Early analytical and experimental work

Modelling the thermal behaviour of pipes in district heating systems, and in thermal networks in the broader sense, has been the subject of scientific studies for a long time already. The work of Esser and Krischer [6] is counted among the first experimental research towards steady state heat losses in pipes with insulation. The mathematical description of the heat loss partial differential equations for a single buried pipe can be found in the work of Carslaw and Jaeger [7]. The first mention of an electrical analogy for the problem is found in D'Eustachio's work [8], leading to the treatment of heat problems with equivalent thermal resistance and capacitance network models. Franz and Grigull [9] described an experimental set-up which allows the study of the heat loss from two pipes as an electrical system and thus explicated the electrical network analogy for the steady state problem in two pipe systems[2].

2.2. Mathematical derivation of steady-state losses

A more formal derivation of the steady state heat losses for dual pipe systems is presented by Wallentén [10], who applied the multipole method to define a symmetric and asymmetric thermal resistance based on the pipes' characteristics. This method has been used earlier to characterise the thermal behaviour of ground heat exchangers in borehole (underground) thermal energy storage systems, for example in the work of Eskilson [11], Bennet et al. [12], Hellström [13] and Claesson and Hellström [14]. Wallentén defined the steady state heat losses by means of a number of shape factors, depending on the configuration of the pipe system. The configuration can consist of single or double pipes, buried underground or in air, and with separate insulation layers or embedded in a common insulation tube. This method will be treated in detail in Section 3.2.

2.3. Operational modelling

The papers described above focus mainly on the description of the heat losses from a static or steady-state point of view. A more operational approach can be found in the work of Benonysson [15], who developed a novel dynamic model for district heating pipes. This model differs from the usual finite volume models in that it treats the propagation of water at a specific temperature and the heat losses separately, while including the thermal capacity of the pipe. Benonysson clearly distinguishes between the so-called *element* model and his new *node* model. The node model splits the transport phenomenon in district heating pipes in three parts:

1. the propagation of fluid with a specific temperature,
2. the thermodynamic behaviour of the pipe due to the pipe wall heat capacity and
3. the steady state heat loss, based on the instantaneous fluid velocity at the outlet.

The *propagation process* determines when the inlet temperature from some point in the past will appear at the outlet, depending on the length of the pipe and the mean fluid velocity in the pipe. This step avoids numerical diffusion that otherwise appears in the element model when the Courant number is not equal or close to one, see also [16]. The *thermodynamic behaviour* and *steady state heat loss* straightforwardly follow from heat transfer theory.

One important assumption in Benonysson's model is that it is sufficient to treat each pipe independently from other adjacent pipes. This was confirmed by Pálsson et al. [16], except for the case of cast concrete pipes. Later, Bøhm and Kristjansson revised this assumption and defined a mutual heat transfer formulation for configurations with double or triple pipes [17]. Further study was conducted by Dalla Rosa et al. [18] who compared the heat losses in detailed simulation models with experimental data and analytical solutions.

Bøhm [19] investigated the dynamic behaviour of buried district heating pipes under changing environmental conditions. The influence of the air temperature is translated to an equivalent boundary temperature at the outermost pipe layer. Comparative studies between commercial software for district heating and the node model are presented by Gabrielaitiene et al. [20], [21]. In these studies, the models were compared with measurement data from different district heating systems. The differences were small as long as the temperature changes were slow and limited, and the variations in mass flow rate were not too high.

The problems of the element model during faster inlet temperature steps and at zero mass flow are recognized by

[2] The idea was first studied by J. Vidal, but this source is irretrievable.

Grosswindhager et al. [22]. Their modified QUICKEST scheme is a variation of the element model that is modified so as to better represent the thermal behaviour during highly dynamic processes. This modification also corrects the erroneous behaviour of the original QUICKEST scheme at pipe junctions or diameter discontinuities.

2.4. Plug flow modelling

Van den Bossche [23] simulated different strategies to provide domestic hot water (DHW) using low temperature thermal networks. One of the considered approaches was to increase the supply temperature for a fixed time frame every day in order to charge a DHW buffer for the rest of the day. However, when using a standard element model, the temperatures at the outlet did not correspond to the expected outcome. Therefore, Van den Bossche proposed a *plug flow model*[3]. The heat losses are calculated based on an equivalent thermal resistance for the pipe and an equivalent water temperature in the pipe, averaging the two fluid parcels in the case of plug flow weighted by their volume. However, still this method does not yield the desired results because of the temperature averaging.

Another analytical solution to the temperature propagation according to the plug flow approach was presented by Jie et al. [24]. The solution for a cyclic input temperature with a period of 24 h was described. The constructed model is applied to a tree-type network in China and the results are in accordance with measurement data. Dalla Rosa et al. [25] validated the node model against a FEM/CFD model. Good correspondence between measurement data, the FEM simulation and the node model was found.

Fang and Lahdelma [26] introduced a least-squares approach to calculate volume flows and heat losses in a tree-like and meshed networks. This method allows accounting for leakages or inconsistencies in the network without stopping the model from functioning. Temperature drops are linearised, as opposed to the exact exponential calculation presented later in the current study. Interaction between the supply and return pipe is included in the total heat loss calculation, but the mutual influence is disregarded because of its small influence. Mixing of multiple streams is accounted for as well.

A novel application of the plug flow approach can be found in the study of Oppelt et al. [27]. In this work, a dynamic thermo-hydraulic model for district cooling networks is presented. The thermal model for single district cooling pipes follows a Lagrangian approach, in which fluid segments in the network are tracked. This model calculates the propagation of temperatures in the pipes as well as the heat flow to and from the surroundings as well as the dissipation of pressure losses in the form of heat. Different from the derivation presented in the Methodology section of this paper, a linear temperature variation between the front and the back of each fluid segment is allowed. The model outcome is compared to reference analytical solutions as well as the outcome of other models. It was found that the plug flow model outperforms most of the existing models.

2.5. New computation tools

The availability of stronger computation tools and better computers also has its influence on pipe models. For example Modelica [28] and Dymola [29] offer new opportunities for the implementation of more detailed and specialized models. One example for heat loss models in district heating pipes is shown by Velut and Tummescheit [30]. They apply a transmission line model to calculate fast dynamics of fluid flows, both regarding pressure and flow phenomena and temperature dynamics. Similarly, Giraud et al. [31] present a library for modelling and simulating district heating systems using the specialized functions that Modelica provides for calculating delays and solving advection equations. The library of Giraud also uses a plug flow approach and is able to reduce the number of equations by almost 97.5%. The numerical result of the models are not completely in line with a validation experiment, but in line with results from other commonly used models. The model is successfully applied to an optimization problem that adapts the supply temperature in order to minimize the heat losses.

2.6. Conclusion from previous studies

This section has given a summary of the gradual development of models for district heating pipes, from the basic heat transfer equations to operational models. It was shown that models that can handle varying inlet temperatures and flow and temperature propagation exist, but to the knowledge of the authors, the mutual influence of the supply and return pipe has not been addressed sufficiently, certainly in the latest generation of fast and accurate simulation models. A motive to reconsider this influence is the growing popularity of twin pipes in the newest generation of thermal networks. This paper aims at filling this gap with an analytical derivation and parameter study.

3. Methodology

The derivation presented below is based mainly on the steady-state heat loss calculation method of Wallentén [10] and the integration of the advection equation over the length of the double pipe system.

3.1. Energy transport equation

The transport of energy through the pipes and the associated heat losses to the surroundings are represented by a combination of the energy and continuity equation [32]:

$$\underbrace{\frac{\partial(\rho u A)}{\partial t}}_{\text{time derivative}} + \underbrace{\frac{\partial\left(\rho v\left(u+\frac{p}{\rho}\right)A\right)}{\partial x}}_{\text{spatial derivative}} = \underbrace{vA\frac{\partial p}{\partial x}}_{\text{pressure difference energy}} + \underbrace{\frac{1}{2}\rho v^2|v|f_D S}_{\text{wall friction dissipation}} + \underbrace{\frac{\partial}{\partial x}\left(kA\frac{\partial T}{\partial x}\right)}_{\text{axial heat diffusion}} - \dot{q}_e, \tag{1}$$

where ρ denotes the mass density, u the specific internal energy, A the cross section area of the pipe, v the flow velocity, p the absolute pressure, x the spatial coordinate along the length of the pipe, t the time, f_D the Darcy friction coefficient, S the pipe circumference, k the thermal conductivity, T the temperature and $\dot{q}_e$ the heat losses

[3] This type of modelling stems from chemical process engineering, where originally the influence of steps in the supply concentrations was studied by means of the plug ow representation.

per unit length. Note that the heat losses as represented by $\dot{q}_e$ are defined to be positive if heat flows from the pipes to the surroundings.

The use of the 1D equation, assuming a uniform water temperature in the pipe cross section, can be justified by evaluating the Nusselt number for different pipe diameters. In the nominal operation conditions advised by pipe manufacturers (e.g., IsoPlus [33]) the lowest *Nu* is found for the narrower pipes and is in the order of 1×10^2, therefore the temperature gradient in the water at the pipe wall is much larger than that from the centre of the pipe to the wall. Furthermore, the heat transfer coefficient from the water to the pipe wall can be found to be much larger than that of the pipe wall to the environment, due to the low conductivity of the insulating material [34]. This adds to the correctness of the 1D heat transfer equation. It is assumed that there is no heat transfer in the axial direction outside the pipe. This is sufficiently accurate because of the low conductivity of ground and insulation and the limited axial temperature gradients.

Neglecting the diffusive heat transport in the pipe is justified when the Péclet number is considerably larger than 1:

$$Pe = \frac{Lv}{k/(\rho c_p)} \gg 1. \tag{2}$$

This criterion depends on a combination of pipe length and flow velocity. Since the diffusivity of water is in the order of magnitude of $1 \times 10^{-7} \mathrm{m}^2/\mathrm{s}$, the product of the flow velocity and the pipe length should be well over this value. Considering that the maximum flow velocities will be between 1 and 5 m/s [34] and the pipe lengths generally encountered in district heating and cooling are in the range of meters and more, it can be assumed that the advection will generally predominate over diffusive heat transfer. During rapid temperature changes, the temperature fronts will of course be somewhat diluted, but in the rest of the paper, steady inlet conditions are assumed.

The dissipation of friction losses in the form of heat are neglected, as is also the case in Refs. [15,31,35,36]. This is less accurate for wider pipes, where the dissipation of the friction losses can actually offset the heat losses, but nevertheless this is not taken into account [34].

Lastly, when realizing that water, in the cases studied, can be assumed incompressible, the variation in internal energy can be written as a function of the temperature variation using the specific heat c_p [37].

$$\frac{\partial(\rho c_p A T)}{\partial t} + \frac{\partial(\rho c_p A v T)}{\partial x} = -\dot{q}_e \tag{3}$$

This equation can be recognised as the advection equation with a source term $-\dot{q}_e$. It can be rather straightforwardly solved using finite volume methods. But as already mentioned, this can become rather resource intensive if high accuracy is needed, and the method introduces discretisation errors, namely numerical diffusion when the Courant number is not equal or close to one.

3.2. Determination of the heat losses per unit length $\dot{q}_e$

This section presents the heat losses per unit length as a function of the temperature in the two pipes at a certain cross section and the boundary temperature. The steady-state heat losses per unit length for double pipe systems are calculated by Wallentén [10]. Depending on the dimensions and material properties, a number of equivalent thermal resistances between the two pipes and the pipes and the undisturbed ground temperature respectively can be calculated. The two pipe lay-outs considered are two pipes in separate insulation (*single pipes*) and two in a common insulating casing (*twin pipes*). Both are presented schematically in Fig. 1.

The heat loss problem is considered as a superposition of two easier problems: one where the pipes only interact with the surroundings and not with each other, i.e. the *symmetrical* problem, and one where the pipes only interact with each other and not with the surroundings, i.e. the *asymmetrical* problem (see Fig. 2). It can easily be checked that when the two component problems are added, the actual situation with supply, return and boundary temperatures results. Notice that the surrounding temperature of the asymmetrical problem is in fact 0° C. This should not be interpreted as an absolute temperature level, but as an offset that is applied to the symmetrical problem. The temperatures in the supply and return pipe in the asymmetrical problem are $\pm T_a$, such that all heat from the supply pipe flows exclusively to the return pipe (and not to the surroundings, since the net heat flux out of the supply pipe is equal to that into the return pipe). For the symmetrical problem, the opposite is true: all heat flows from the pipes to the surroundings, no heat is exchanged between the pipes.

Irrespective of the lay-out choices, the heat losses are calculated as the combination of the symmetrical and asymmetrical heat transfer problem:

$$\dot{q}_s = \frac{T_s - T_b}{R_s} \text{ where } T_s = \frac{T_v + T_r}{2} \tag{4}$$

$$\dot{q}_a = \frac{T_a}{R_a} \text{ where } T_a = \frac{T_v - T_r}{2} \tag{5}$$

$$\dot{q}_v = \dot{q}_s + \dot{q}_a \tag{6}$$

$$\dot{q}_r = \dot{q}_s - \dot{q}_a \tag{7}$$

where $\dot{q}$ denotes the heat losses per unit length, R the thermal resistance per unit length (in Km/W) and T the temperature. The subscript s points to the symmetrical and a to the asymmetrical heat loss problem; v refers to the supply pipe, r to the return pipe. For better understanding of (4)–(7), the equations can be represented graphically in an equivalent thermal resistance model (see Fig. 3). This model combines the asymmetrical and symmetrical heat losses in one single figure.

As to the correctness of the assumption of steady-state heat losses, it suffices to realise that the product of the thermal capacity of the material surrounding the pipe and the temperature variations of this material is negligible with respect to the energy change of the water that flows in the pipes [15]. In a later step, the effect of the wall and insulation capacity may be added for accuracy, but its

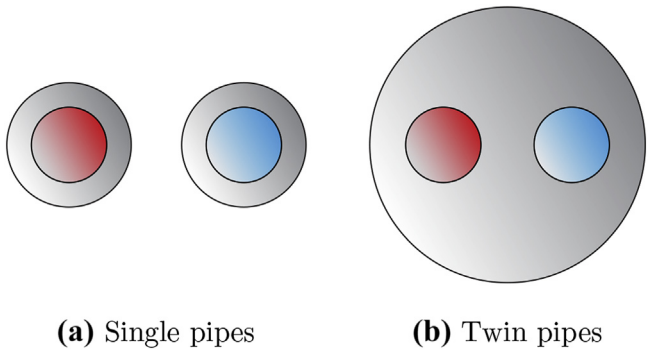

Fig. 1. Schematic representation of the types of double pipes considered in this study.

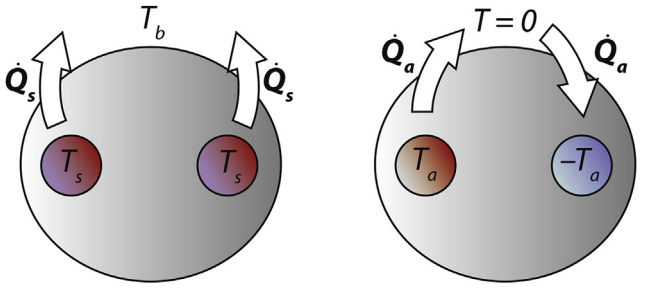

(a) Symmetrical heat losses **(b)** Asymmetrical heat losses

Fig. 2. Components of the heat loss problem.

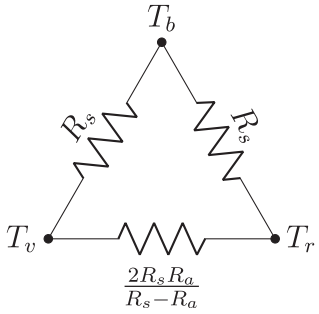

Fig. 3. Equivalent resistance model.

effect remains limited, even for varying inlet temperatures.

3.3. Formulation of heat loss problem along the pipe

Realising that the axial diffusion in the studied problem is negligible (see section 3.1), the temperature change of a specific parcel of fluid mainly depends on its initial temperature at the inlet, the temperature of the surroundings, i.e. the temperatures in the opposite pipe and the undisturbed ground temperature, and on the time that it remains in the pipe. The degree of mutual influence of the supply and return pipe depends on the proximity and lay-out of the pipe system. As mentioned earlier, the lay-out only affects the values of the resistances in the heat loss equations, and hence does not influence the mathematical formulation of the solution.

In existing networks, mostly pipe systems with equal diameters for supply and return are encountered. Usually the mass flows in the supply and return line are equal and opposite in each network segment. This case will be referred to as cross flow. Parallel flow can occur as well, typically in ring-type networks [38,39]. However, in this type of district heating systems the mass flow rates for supply and return may differ in the same cross section; hence, the diameters of supply and return side may differ as well to minimise pumping power. Due to these additional variables, the parallel flow case requires a different solution, so only the cross flow lay-out is considered in the rest of the paper.

To calculate the temperature profile in both pipes, the energy balance equation (3) is completed with an expression for the temperature-dependent heat losses (see Fig. 3). This equation must be transformed from a PDE to an ODE to solve analytically, therefore the assumption of a steady-state solution must be made. The dynamic behaviour can be represented additionally by changing the inlet temperature accordingly. Additionally, a constant velocity v is assumed. It will be seen that the velocity does in general not have a large influence on the result, hence this assumption is valid. Finally, the undisturbed ground temperature T_b is constant under the steady-state assumption. Also for dynamic cases, the change of the soil temperature is expected to be considerably slower than the changes of temperatures in the pipe and hence their dynamics can be neglected.

Recognising that this yields two equations (for supply and return side), the following system of ordinary differential equations can be constructed:

$$\begin{cases} -Cv\dfrac{\partial T_v}{\partial x} = T_v\left(\dfrac{R_a+R_s}{2R_sR_a}\right) + T_r\left(\dfrac{R_a-R_s}{2R_sR_a}\right) - \dfrac{T_b}{R_s} \\ -C(-v)\dfrac{\partial T_r}{\partial x} = T_r\left(\dfrac{R_a+R_s}{2R_sR_a}\right) + T_v\left(\dfrac{R_a-R_s}{2R_sR_a}\right) - \dfrac{T_b}{R_s} \end{cases} \tag{8}$$

Notice the negative sign of the velocity in the return pipe equation. Since v is assumed to be positive when the flow in the supply pipe proceeds in the positive x direction, the minus sign is needed to account for the opposite flow direction in the return pipe. If the flow reverses, this leads to a negative value of v. For reversing flow, the inlet and outlet (see next section) must be interchanged as well.

3.4. Temperature profile along the pipe and determination of temperature change

This system of equation (8) can be integrated between $x = 0$ and $x = L$ (length of the pipe ensemble), involving a somewhat tedious derivation. By imposing inlet conditions on the supply and return pipe ($T_v(x = 0) = T_{v,in}$ and $T_r(x = L) = T_{r,in}$), the temperature profile for both pipes as a function of the axial position can be found:

$$T_v(x) = -\xi(x)\frac{(R_s+R_a-2\sqrt{R_sR_a})(T_{v,in}-T_b) - \xi_L(R_s-R_a)(T_{r,in}-T_b)}{\xi_L^2(R_s+R_a+2\sqrt{R_sR_a}) - (R_s+R_a-2\sqrt{R_sR_a})} + \xi(-x)\frac{\xi_L^2(R_s+R_a+2\sqrt{R_sR_a})(T_{v,in}-T_b) - \xi_L(R_s-R_a)(T_{r,in}-T_b)}{\xi_L^2(R_s+R_a+2\sqrt{R_sR_a}) - (R_s+R_a-2\sqrt{R_sR_a})} + T_b \tag{9}$$

$$T_r(x) = -\xi(x)\frac{(R_s-R_a)(T_{v,in}-T_b) - \xi_L(R_s+R_a+2\sqrt{R_sR_a})(T_{r,in}-T_b)}{\xi_L^2(R_s-R_a+2\sqrt{R_sR_a}) - (R_s+R_a-2\sqrt{R_sR_a})} + \xi(-x)\frac{\xi_L^2(R_s-R_a)(T_{v,in}-T_b) - \xi_L(R_s+R_a-2\sqrt{R_sR_a})(T_{r,in}-T_b)}{\xi_L^2(R_s-R_a+2\sqrt{R_sR_a}) - (R_s+R_a-2\sqrt{R_sR_a})} + T_b \tag{10}$$

In these equations, the following substitution is used to condense the expressions somewhat [4]:

$$\xi(x) = \exp\left(\frac{x}{vC\sqrt{R_s R_a}}\right) \tag{11}$$

and

$$\xi_L = \exp\left(\frac{L}{vC\sqrt{R_s R_a}}\right) \tag{12}$$

To know the outlet temperature of the supply and return pipe, the expression for T_v is evaluated at $x = L$ and for T_r at $x = 0$:

$$T_v(L) = \frac{4\xi_L\sqrt{R_a R_s}(T_{v,in} - T_b) + \left(\xi_L^2 - 1\right)(R_s - R_a)(T_{r,in} - T_b)}{\xi_L^2(R_s + R_a + 2\sqrt{R_s R_a}) - (R_s + R_a - 2\sqrt{R_s R_a})} + T_b \tag{13}$$

$$T_r(0) = \frac{4\xi_L\sqrt{R_a R_s}(T_{r,in} - T_b) + \left(\xi_L^2 - 1\right)(R_s - R_a)(T_{v,in} - T_b)}{\xi_L^2(R_s + R_a + 2\sqrt{R_s R_a}) - (R_s + R_a - 2\sqrt{R_s R_a})} + T_b \tag{14}$$

(13) and (14) show that, as expected, the temperature change depends on the boundary temperatures, the insulation and dimensions of the pipe and the delay time. This last parameter appears in the ratio of the length of the pipe and the fluid velocity. From this ratio, it follows that for large enough fluid velocities, the solution becomes approximately independent of changes in the velocity.

A parallel between the time constant of a dynamical heat transfer problem and the denominator in the argument of the exponential terms can be recognized, after substituting or L/v by the time delay. Since the equations in system (8) are of second order, there are two characteristic solutions. In this problem, the roots are opposite but equal in absolute value (see $\xi(x)$ and $\xi(-x)$). In this equivalent "time" constant $C\sqrt{R_s R_a}$ (since the solution assumes a steady state, the time refers rather to the time delay, changing with the flow velocity), two contributions can be recognized: the "time" constant of the asymmetrical (15) and that of the symmetrical problem (16), averaged geometrically in (17). This final equation can be found in (11) and (12).

$$\tau_a = R_a C \tag{15}$$

$$\tau_s = R_s C \tag{16}$$

$$\tau = \sqrt{\tau_a \tau_s} = C\sqrt{R_s R_a} \tag{17}$$

3.5. Implementation of heat loss model

The equations derived in the previous section can be implemented in an equation-based modelling language such as Modelica. The requirement is that the language can solve an advection equation in order to model the propagation of water of a specific temperature through the pipes. Modelica offers the `spatialDistribution()` function for this. The advective transport is treated separately from the heat losses, which are applied at the exit of the pipe, taking into account the temperature boundary conditions and the transport delay. A third independent phenomenon that can be included is the capacity of the pipe wall and insulation. Hence, the steady-state solution can be applied for varying inlet temperatures, too.

An implementation of the model can be found in the IEA-EBC Annex 60 Modelica library for buildings and community energy systems (for a general description of this library, see Ref. [40]). Of course, the use of Modelica or even equation-based languages is not a requirement. These equations can be implemented in any programme that is able to represent the advection in an adequate way.

Since this paper focuses on the steady-state solution, the solution from 3.4 is implemented in Python for further parameter study.

4. Results

This section describes the results that follow from the derivations presented in the Method section (3, equations (13) and (14)). The focus lies on determining the factors that influence heat losses in double pipe lay-outs. The parameters that are considered in this study are: mass flow rate, pipe diameter, and temperature levels in supply and return. The pipe length is not studied since it is a trivial result that increasing the length will increase heat losses proportionally.

All dimensions and materials for the calculation of the heat transfer parameters are derived from the IsoPlus catalogues [33]. For separately insulated pipe systems, the minimal installation distance stipulated by the producer is respected. Hence, the mutual influence between supply and return as presented in this paper serves as a worst-case scenario to be expected from correctly installed pipes.

4.1. Influence of mass flow rate on heat losses

Fig. 4 shows the outlet temperatures for a twin pipe system in common insulation (see Fig. 1b) together with the inlet temperature (solid lines). The inlet temperature of the supply side is 60°C, at the return side it is 30°C. The undisturbed ground temperature is 5°C. The pipes have a length of 1 km. The pipes have a diameter of DN50 (50 mm) and are buried 2 m underground.

From Fig. 4, it is clear that for high enough mass flow rates (for this example, $\dot{m} > 3$ kg/s or $\Delta t < 11$ min), the outlet temperature is approximately equal to the inlet temperature, at least for this DN50

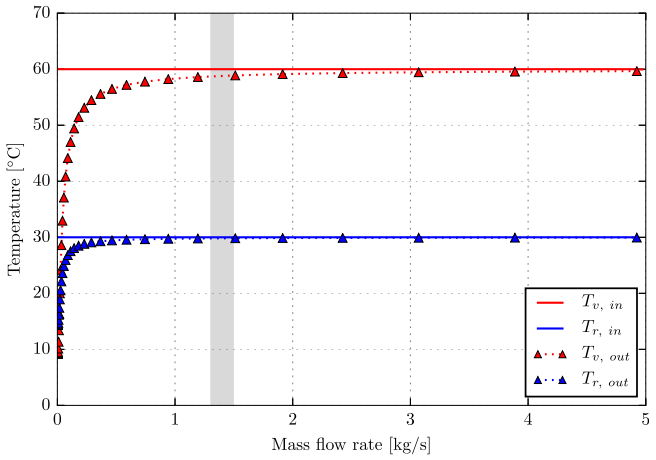

Fig. 4. Outlet temperature of DN50 double pipe (common insulation) of 1 km as a function of mass flow rate. The grey area denotes the economic mass flow rate range as suggested by IsoPlus [33].

[4] Note that $\xi(-x) = 1/\xi(x)$ due to the exponential expression.

pipe and length of 1 km. Fig. 4 shows that the advised mass flow rate for a DN50 pipe is actually below this limit. Notice however that such narrow pipes will usually not be installed to transport heat over such large distance. The smaller value of L in the exponential term in (13) and (14) will make sure that the outlet temperature approaches the inlet temperatures much closer at lower mass flow rates. A further discussion of the influence of the mass flow rate for different pipe diameters can be found in section 4.3.

In other words, the temperature drop is negligible and the steady-state heat losses per length of Wallentén can be applied along the pipe. Only for very small mass flow rates (where $\xi_L \gg 1$), the outlet temperature starts to drop at the supply side. At the return side, the drop is less outspoken because of the heat that it receives from the supply side.

The heat losses from supply and return side for the entire pipe length can be calculated as follows:

$$\dot{Q}_v = \dot{m}c_p \cdot (T_{v,in} - T_{v,out}) \quad \text{and} \tag{18}$$

$$\dot{Q}_r = \dot{m}c_p \cdot (T_{r,in} - T_{r,out}), \tag{19}$$

where $T_{r,out}$ and $T_{v,out}$ are calculated as in (13) and (14). These heat losses are shown in Fig. 5 as blue and red dots for respectively the return and supply pipe. The dashed line shows the sum of these losses, hence the total losses for the entire pipe system. Alternatively, the heat losses can be calculated by multiplying the heat losses from (6) and (7) with the pipe length L, resulting in $\dot{Q}_{v,Wall}$ and $\dot{Q}_{r,Wall}$ from Fig. 5.

It is clear from Fig. 5 that the heat losses as calculated from the actual temperatures at the in- and outlets and the mass flow rates are nearly the same as those calculated using the steady state losses from Wallentén. Furthermore, the heat losses are nearly independent of the mass flow rate for high enough mass flow rates (see above).

Comparing Figs. 4 and 5 closely, it may seem contradictory how the outlet temperature and the heat losses of the return pipe evolve in the opposite direction for low mass flow rates. This relative increase is caused by the heat that is transferred from the hot pipe to the cold pipe, and subsequently dissipated to the environment. If the return temperature were even lower, this becomes evident since the heat losses for the return pipe are negative. However, for mass flow rates close to zero, the heat losses are limited by the total heat actually supplied to the pipe (calculated as $\dot{m}c_p(T_{v,in} - T_{r,out})$). In the transition region between the intuitive region (heat losses for both pipes positive and monotonously increasing with mass flow) and the region where the return losses are negative, this transition with non-monotonous heat losses as a function of the mass flow rate appears. For even lower mass flow rates, the heat losses for both sides approach zero.

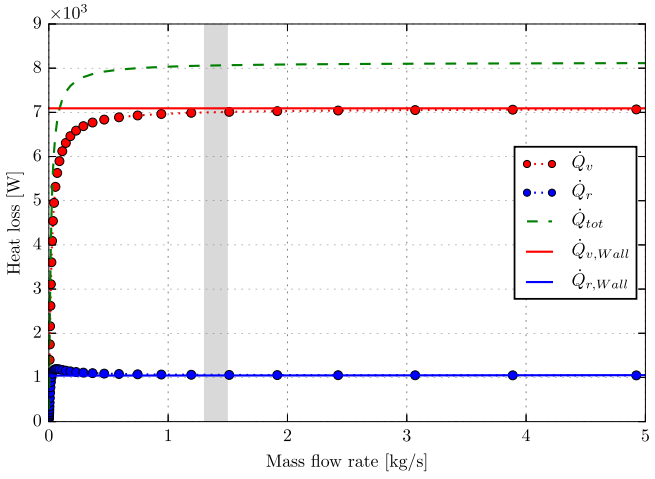

Fig. 5. Heat losses of DN50 double pipe (common insulation) of 1 km as a function of the mass flow rate. The grey area denotes the economic mass flow rate range as suggested by IsoPlus [33].

4.2. Influence of pipe dimensions and temperatures

In the previous section, it has been shown that for high enough mass flow rates, the heat losses may be treated as a constant value, at least with respect to the mass flow rate. The value of the heat losses can be approximated using the simple formulas proposed by Wallentén (4)–(7). In this section, other influences on the heat losses are studied, more precisely the influence of the temperature levels in the pipes and the dimensions.

Revisiting the expressions for the steady state heat losses as defined by Wallentén, the importance of the asymmetrical heat losses with respect to the symmetrical losses can be determined as follows: the total heat losses ($\dot{q}_v + \dot{q}_r = 2\dot{q}_s$) are independent of the asymmetrical heat loss problem, not influenced by the degree of mutual interaction between supply and return. Hence, it can be derived that the ratio of heat transfer from the supply to the return side is proportional to the ratio of $\dot{q}_a/\dot{q}_s$, omitting constant factors:

$$\frac{\dot{q}_a}{\dot{q}_s} = \frac{T_a}{T_s}\frac{R_s}{R_a} \propto \frac{T_v - T_r}{T_v + T_r - 2T_b}\frac{h_a}{h_s}; \tag{20}$$

the terms h_a and h_s are the so-called *shape factors* and they can be calculated as described by Wallentén [10]. They influence the resistance of both the symmetrical and asymmetrical problem according to the following expression:

$$R = \frac{1}{2\pi k h}, \tag{21}$$

where k can be (depending on the case) the thermal conductivity of the insulation material or the ground. The value itself is assumed to be constant and homogeneous and is omitted from the scale analysis. The shape factor depends purely on the pipes' geometry. From (20) it is clear that the mutual influence of the two pipes on each other is a function of the temperatures at the inlet and the boundary of the pipe system and of its geometry.

The influence of the pipe geometry is displayed in Fig. 6. Of

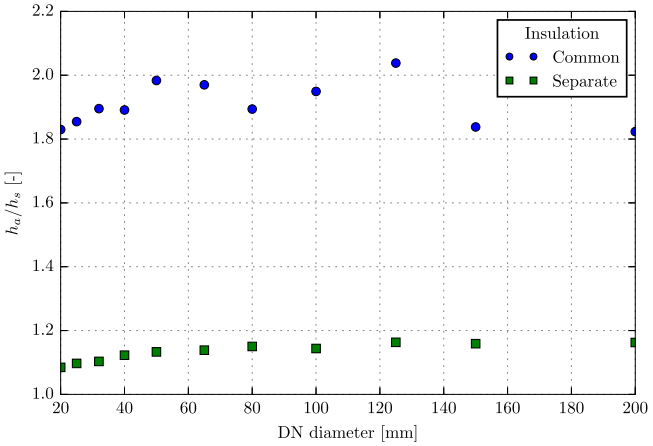

Fig. 6. Evolution of h_a/h_s -ratio for different pipe sizes and for separate insulation (pipes at minimal installation distance) and common insulation.

course, this is not an exhaustive representation; instead of checking the sensitivity with respect to all geometric parameters (e.g. buried depth, distance between the pipes, wall thickness, insulation thickness), the evolution for different pipes within the diameter range DN20 to DN200 is displayed. The pipes considered are taken from the IsoPlus catalogue [33]. The twin pipes are standard pipes, the single pipes are 1x reinforced (thicker materials and hence better insulating properties than the standard single pipes).

Although there is some variation in the ratio, it is clear that within the two product ranges (twin pipes and separate pipes) the ratio remains in a narrow range for different diameters. This is undeniably a design choice, but this means that for this type of pipes the mutual influence for the same pipe lay-out remains approximately the same.

It is however clear that the heat ratio $\dot{q}_a/\dot{q}_s$ for the same temperature levels will be significantly higher for twin pipes than for separately insulated pipes. This does not imply that the twin pipes are less efficient, since the total heat losses $(\dot{q}_v + \dot{q}_r)$ are much lower for the twin pipe layout than for the separately insulated pipes. This effect is illustrated in Fig. 7 for the same temperatures as in Figs. 4 and 5 ($T_v = 60°C,\ T_r = 30°C,$ and $T_b = 5°C$).

The second group of parameters that influences the mutual interaction of the pipes is, as seen in (20), that of the inlet and boundary temperatures. This factor will be represented by the temperature ratio ϑ, defined as follows:

$$\vartheta = \frac{T_v - T_r}{T_v + T_r - 2T_b} \tag{22}$$

In the numerator of ϑ, the temperature difference between supply and return appears. This corresponds to the intuition that the amount of heat that flows from the supply to the return side is larger for a higher temperature difference than that for a small difference (with exactly 0 W of heat transfer for equal temperatures at the two sides).

In the denominator of ϑ, we find the sum of the two pipe temperatures. From this value, the double boundary temperature is subtracted. As such, this term can be regarded as the difference between the average temperature and the surroundings multiplied by two. Again, this could be expected intuitively: the higher the average pipe temperature is with respect to the ground temperature, the more heat is lost and the smaller the net influence of the mutual heat exchange between the pipes. On the other hand, when the average temperature of the pipes is the same as that of its surroundings, no heat is lost from the ensemble of the pipes, but instead all heat transfer will be from the hot to the cold pipe. In this case, the heat ratio is a division by zero. Indeed, when the total heat loss is zero, the importance of the mutual heat transfer becomes undefined.

The evolution of the temperature ratio ϑ for variations of the temperature difference and of the supply temperature are shown in Fig. 8. Here, it is clear that the mutual influence, quantified by the temperature ratio ϑ, indeed decreases for increasing supply (or by proxy, average) temperature levels. At the same time, the mutual influence becomes more pronounced for higher temperature differences between supply and return. Given the trend towards lower network temperatures and increased ΔT, it seems important to take the mutual influence into account.

4.3. Influence of mass flow rate for different pipe diameters

Fig. 9 is a combination of the analyses performed in the previous sections. In the first place, it shows the heat losses as calculated

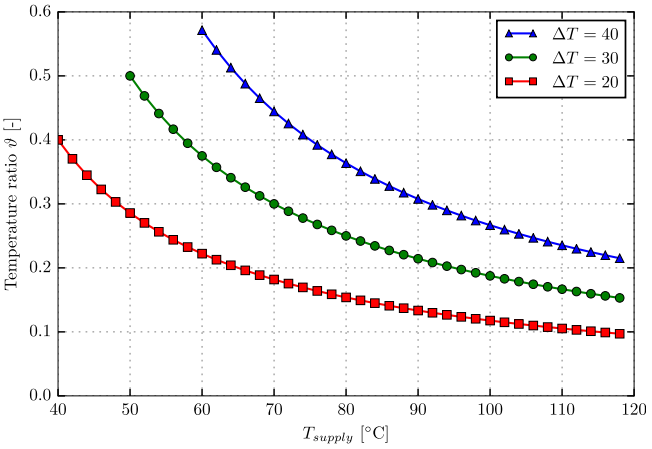

Fig. 8. Comparison of the temperature ratio influence for different supply temperatures and three temperature differences between supply and return side. The boundary temperature T_b is fixed at 5°C.

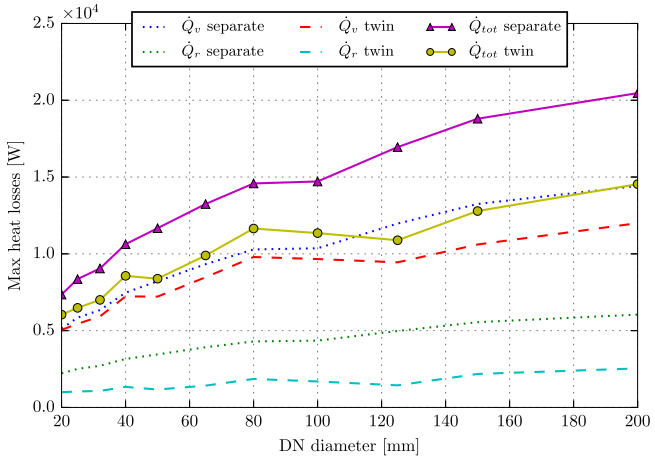

Fig. 7. Comparison between supply, return and total heat losses for separately insulated and twin pipes for different diameters for 1 km pipe length.
*Note:*The pipes considered are taken from the IsoPlus catalogue [33]. The twin pipes are standard pipes, the single pipes are 1x reinforced.

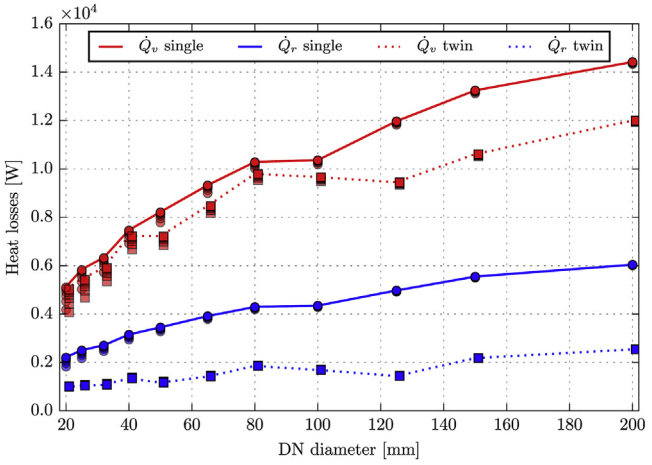

Fig. 9. Comparison of influence of mass flow rate and pipe diameter on the heat losses for single and twin pipes. The lines show the heat losses as calculated with Wallentén's method.
Note: the squares (heat loss i.f.o. mass flow rate for twin pipes) have been offset slightly horizontally in order to be able to distinguish them better from the circles.

with Wallentén's method using the pipe lay-out and temperatures from the previous analyses (solid and dotted lines for separate and twin pipes respectively). Furthermore, the squares and circles show the variation in heat losses for a range of fluid velocities between 0.1 m/s and 10 m/s[5], for the twin and single pipes respectively. Fig. 9 shows that the range due to varying velocity for the supply side is more or less the same for single and twin pipes. At the return side though, the losses for the twin pipe configuration seem to be less influenced by the flow velocity (or equivalently, the mass flow rate). Furthermore, it is noteworthy that for both configurations, the influence of flow velocity on the heat losses diminishes with increasing pipe diameter.

This can be appreciated rewriting (13) and (14) by substituting v with $\dot{m}/(A\rho)$. Furthermore, with $C = A\rho c_p$ it is found that the argument of the exponential ξ_L can be replaced by $L/(\dot{m}c_p\sqrt{R_s R_a})$. This expression is largely independent of the pipe diameter, except for the slight decrease of the resistances R_s and R_a with the pipe diameter (see Fig. 10; the resistance scales linearly with the inverse shape factor). At the same time, the "economic mass flow rate range" increases quadratically with the diameter (Fig. 11).

Considering that the rest of the argument of ξ_L stays approximately the same, as well as the rest of the solutions, it can be seen that for different diameters, more or less the same outlet temperature as a function of the mass flow rate can be used, except that the working range will shift towards higher mass flow rates for higher diameters. This is illustrated in Fig. 12[6]. The difference of the outlet temperatures with respect to the inlet temperatures is actually smaller for narrower pipes, due to larger values of R.

Because of the higher mass flow rates in larger pipes, the deviation from the heat losses as calculated with Wallentén's method will decrease for bigger pipes. For the smaller pipes (DN20–DN50), the error is larger. However, these smaller diameters are, as mentioned earlier, usually only installed for shorter branches. Hence, the temperature difference between inlet and outlet decreases again such that the model is accurate for the expected mass flow rate range.

4.4. Verification of heat losses

In this section, the heat losses calculated with Wallentén's method, found to be the approximately correct value over a large range of mass flow rates, are compared with values given in the IsoPlus catalogue [33]. The IsoPlus catalogues for double pipes stipulate the heat losses per unit length of pipes for several *average temperature differences*. This is similar to the treatment of temperatures in Wallentén's method, where the total losses depend on the average temperature of supply and return, compared to the ground temperature; this temperature is referred to as

$$T_M = \frac{T_v + T_r}{2} - T_b. \tag{23}$$

For this comparison, an average temperature difference T_M of 80 K has been chosen. For the regime used in the earlier examples in this paper, T_M would amount to $\frac{60+30}{2} - 5 = 40$ K. However, heat losses for this T_M were not provided by IsoPlus. Furthermore, the buried depth of the pipes is 0.8 m in this case, whereas for the other analyses in this paper a value of 2 m has been used.

Fig. 13 plots the differences between the IsoPlus catalogue losses and those calculated using Wallentén's method. The grey band represents a ±5% interval around the catalog data. For pipes above DN50, the heat losses as calculated by this paper lie within the 5% band. For the lower pipe diameters, the calculation is further off,

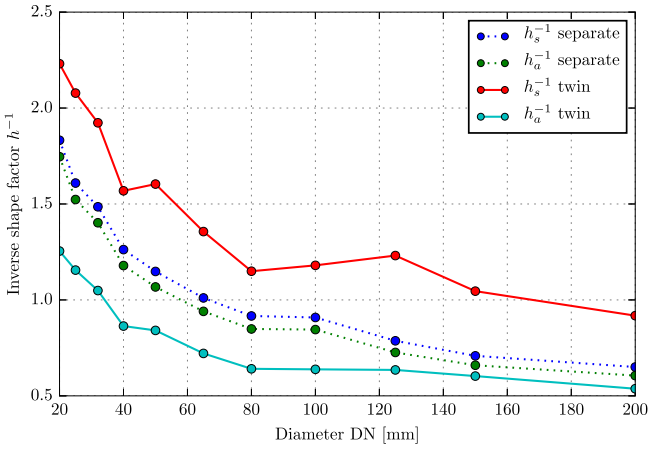

Fig. 10. Evolution of the inverse shape factor (h^{-1}) for separate pipes and twin pipes as a function of the pipe diameter. Calculation following Wallentén's method [10] with measurements from the IsoPlus catalogue [33].

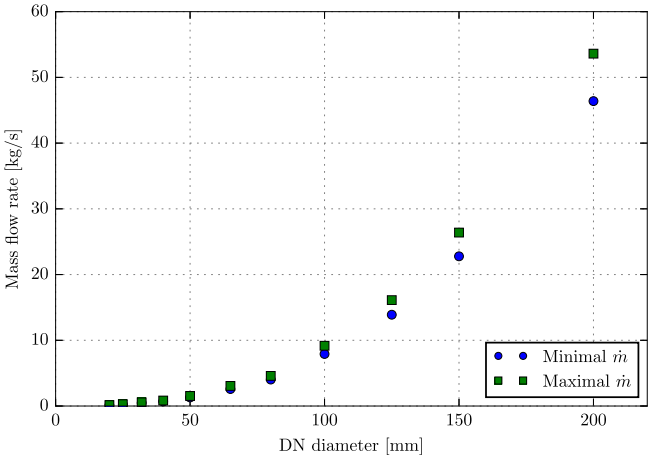

Fig. 11. Advised mass flow rate range per pipe diameter according to IsoPlus [33].

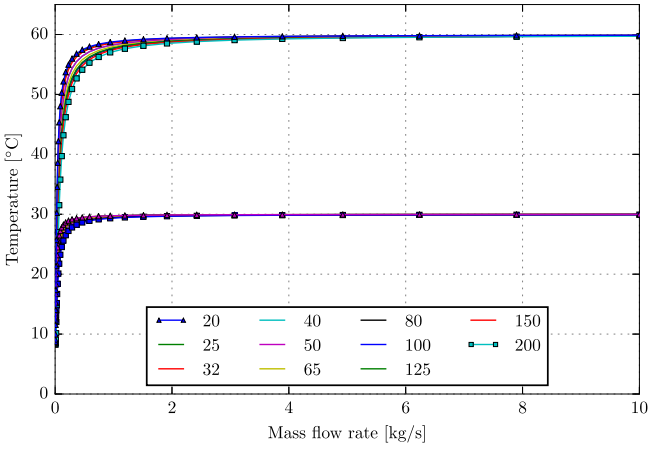

Fig. 12. Variation of the supply and return outlet temperature as a function of the mass flow rate for different pipe diameters. Values for $T_{v,in} = 60\,^{\circ}\mathrm{C}, T_{r,in} = 30\,^{\circ}\mathrm{C}, T_b = 5\,^{\circ}\mathrm{C}$ and a pipe length of 1 km.

[5] The velocities are equidistant on a logarithmic scale.

[6] The actual outlet temperatures in this figure are not so important as the visualization of the similarity of the results for different diameters.

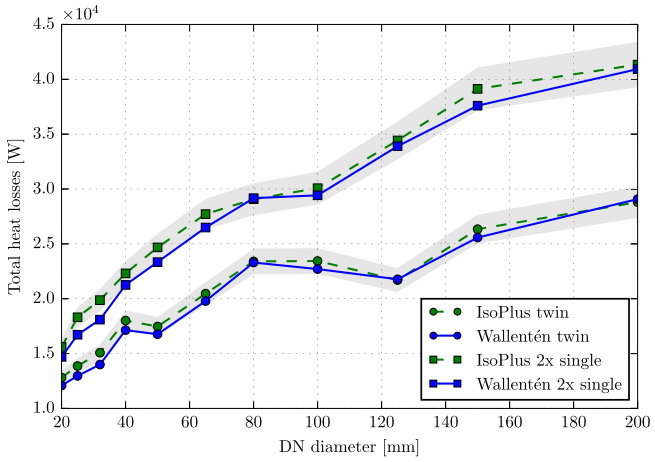

Fig. 13. Comparison of total heat losses from the IsoPlus catalogue [33] for $T_M = 80$ K and using Wallentén's method ($T_v = 90^\circ$C, $T_r = 70^\circ$C and $T_b = 0^\circ$C) for a pipe length of 1 km. The grey bands show a ±5% interval around the catalog data.

but the trend of the catalog data is still followed. The exact calculation methods or measurements at IsoPlus are not known and this may explain the slight differences that are present. IsoPlus does not supply a measure of accuracy for their values.

4.5. Comparison of separately insulated pipes modelled jointly and separately

In this subsection, the influence of (not) taking the mutual heat transfer into account is established. Fig. 14 shows the heat losses for a kilometre of pipes with separate insulation. The losses have been calculated twice: once with the assumption of no interaction between the pipes (as mentioned in Refs. [15,16]), and once with the coupled method derived in this paper.

For the solution without coupling, the calculation of the heat losses is limited to that of a cylindrical insulation between the actual pipe temperature (different value for supply and return) and the undisturbed ground temperature T_b. Indeed, the heat loss for a single buried pipe with cylindrical insulation is also described by Wallentén [10]. This calculation boils down to a cylindrical thermal resistance with a correction factor to account for the fact that the pipe is buried in the ground. In Fig. 14, these heat losses as a function of the pipe diameter (using the minimum installation distance as advised by the producer) are shown in the two dotted lines, again using the 60/30°C regime and pipes of 1 km. These heat losses are calculated for a high enough mass flow rate (such that $\xi_L \approx 0$, $\dot{m} > 3$ kg/s for the DN50 pipe of 1 km), such that the heat loss per unit length can simply be calculated using the steady-state heat loss equation for a single pipe.

The solid lines represent the heat losses using Wallentén's equations for the coupled problem. The discrepancy between the heat losses for the two solution strategies is clear and illustrates the necessity of accounting for the mutual influence of the supply and return side of the pipes.

In the lower part of Fig. 14, the relative difference in the heat loss is visualized. The largest difference appears in the return pipe, where a value of up to 10% is encountered. For the supply pipe, the relative and absolute difference are smaller.

For twin pipes, it is impossible to separate the behaviour of the supply and return pipe. Trying to do so involves using eccentrically positioned cylindrical thermal resistances. However, since both of them occupy the same space, it hardly makes sense to treat them separately. Therefore, this comparison is not treated in further detail here. The authors believe it is sufficient to realise that the mutual influence is larger in twin pipes than in single pipes, so since it was concluded earlier that accuracy may be improved in single pipes by accounting for the mutual heat transfer, this must certainly be the case for twin pipes.

5. Discussion

It has been shown that the influence of the mass flow rate on the actual temperature drop is rather low. Only for very low fluid velocities the temperature drop increases, in particular for the pipe with the largest temperature difference with regard to the surroundings. On the other hand, it can be verified that the relative importance of the heat losses with respect to the effectively transmitted heat, although not much different in absolute value, increases greatly in these low mass flow rate regimes. It can thus be argued that the regime with low mass flow rates will be less relevant to the normal application range of the model because of the high proportional losses, although the analytic solution will still be valid.

Since the model will mostly be used in regimes where the

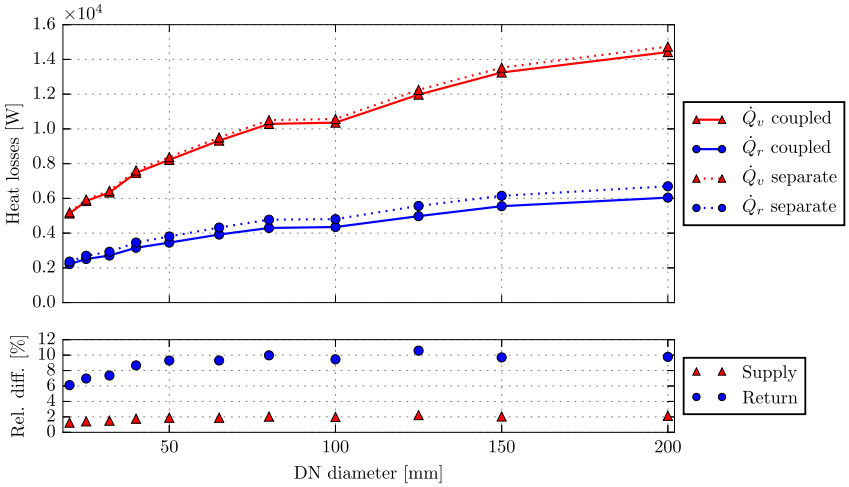

Fig. 14. Comparison of separately insulated pipes, modelled independently and with the coupled equations for a pipe length of 1 km. The relative differences (with the coupled solution as reference) are shown in the lower graph.

temperature drop is nearly independent of the mass flow rate, it may be linearised with respect to the mass flow rate for a specific temperature regime. In other words, the heat losses can be assumed to be a function of the pipe geometry and the temperature levels at the supply and return side only. Particularly with regard to design and operational optimization problems, this is a very interesting result, since heat losses can be treated as a function of the pipe dimensions and the temperature levels only.

6. Conclusion

In this paper, the mathematical derivation of the steady-state heat losses and temperature changes for double thermal network pipes has been presented. Based on the work of Wallentén [10] and Benonysson [15], the derivation is aimed at correctly integrating the heat losses along the pipes such that an accurate steady-state temperature profile can be obtained.

A parameter analysis of the model has shown that the heat losses are nearly independent of the mass flow rate, except for relatively low mass flow rates. The exact boundary depends on the length and diameter of the pipes. The influence of the mass flow rate at low values on the heat losses even decreases with increasing pipe diameters.

Furthermore, the influence of the temperature levels and pipe dimensions on the importance of heat losses from the supply pipe to the return pipe has been investigated. It is concluded that for the specific pipe dimensions of one producer, the diameter is of little influence, but the temperatures are an important factor. The total heat losses calculated with the model developed have been found to be in accordance with nominal heat loss values provided by the producer.

Finally, incorporating the mutual influence of supply and return side leads to higher accuracy in the heat loss calculations, even more so for the case of lower average network temperatures. Together with the analytical derivation that the heat losses can be assumed independent of the mass flow rate, this is an interesting result for further research towards the optimal design and operation of thermal networks.

As an outlook towards further research, the proposed solution could be implemented in a dynamic model. The accuracy could be checked either with detailed simulations in CFD/FEM software, or by employing an experimental setup. Furthermore, the potential of the linearised heat loss equations should be checked in design and operational optimization problems for thermal networks.

Acknowledgement

The authors gratefully acknowledge EFRO/SALK and IWT/VLAIO for funding the research work of Bram van der Heijde and Arnout Aertgeerts through the projects ‘Towards a Sustainable Energy Supply in Cities’ and IWT Proeftuin ‘De Schipjes’. The former receives the support of the European Union, the European Regional Development Fund ERDF, Flanders Innovation & Entrepreneurship and the Province of Limburg (EFRO SALK project 936), the latter from IWT/VLAIO (Project 140125, IWT PROEFTUIN ‘Woningrenovatie: innovatie bij energiezuinig verbouwen’). The work of Bram van der Heijde is co-financed by VITO through a PhD Fellowship.

References

[1] Lund Henrik, Werner Sven, Wiltshire Robin, Svendsen Svend, Eric Thorsen Jan, Hvelplund Frede, et al. 4th Generation District Heating (4GDH). Integrating smart thermal grids into future sustainable energy systems. Energy 2014;68:1–11. http://dx.doi.org/10.1016/j.energy.2014.02.089. ISSN 03605442, http://dx.doi.org/10.1016/j.energy.2014.02.089.

[2] Connolly David, Nielsen Steffen, Persson Urban. Heat Roadmap Europe 2050. Aalborg: Department of Development and Planning, Aalborg University; 2013, ISBN 9788791404481.

[3] Persson U, Möller B, Werner S. Heat Roadmap Europe: identifying strategic heat synergy regions. Energy Policy Nov 2014;74:663–81. http://dx.doi.org/10.1016/j.enpol.2014.07.015. ISSN 03014215, http://linkinghub.elsevier.com/retrieve/pii/S0301421514004194.

[4] European Commission. Communication from the commission to the european parliament, the council, the european economic and social committee and the committee of the regions on an EU Strategy for heating and cooling. Technical report. Brussels: European Commission; 2016a. https://ec.europa.eu/energy/sites/ener/files/documents/1/_EN/_ACT/_part1/_v14.pdf.

[5] European Commission. Communication from the commission to the european parliament, the council, the european economic and social committee and the committee of the regions on an EU Strategy for heating and cooling - review of available information. Technical report. Brussels: European Commission; 2016b. https://ec.europa.eu/energy/sites/ener/files/documents/1/_EN/_autre/_document/_travail/_service/_part1/_v6/_0.pdf.

[6] Esser W, Krischer O. Die Berechnung der Anheizung und Auskühlung ebener und zylindrischer Wänder. Berlin: Springer-Verlag Berlin Heidelberg; 1930, ISBN 9783662314371.

[7] Carslaw HS, Jaeger JC. Conduction of heat in solids. Oxford. 2e ed. Clarendon: Oxford; 1984. tenth ed., 1984.

[8] D'Eustachio D. Criteria for thermal insulation for use on underground piping. In: Symposium on thermal conductivity measurements and applications of thermal insulations. Philiadelphia, PA: American Society for Testing Materials; 1957. p. 81–6. https://books.google.com/books%3fid%3dOf44rreit9UC%7b%26%7dpgis%0d1.

[9] Franz G, Grigull U. Wärmeverluste von beheizten Rohrleitungen im Erdboden. Heat Mass Transf 1969;2(2):109–17. http://www.springerlink.com/index/Q583385587413M61.pdf.

[10] Wallentén Petter. Steady-state heat loss from insulated pipes. PhD thesis. Sweden: Lund Institute of Technology; 1991.

[11] Eskilson P. Thermal analysis of heat extraction boreholes. PhD thesis. University of Lund; 1987.

[12] Bennet J, Claesson J, Hellström G. Multipole method to compute the conductive heat flows to and between pipes in a composite cylinder. Notes Heat Transf January, 1987;3:3–42. http://lup.lub.lu.se/record/1894632/file/1894641.pdf.

[13] Hellström Göran. Ground heat storage - thermal analyses of duct storage systems. PhD thesis. University of Lund; 1991.

[14] Claesson Johan, Hellström Göran. Multipole method to calculate borehole thermal resistances in a borehole heat exchanger. HVAC&R Res 2011;17(6):895–911. http://dx.doi.org/10.1080/10789669.2011.609927. ISSN 10789669, http://www.tandfonline.com/doi/abs/10.1080/10789669.2011.609927.

[15] Benonysson A. Dynamic modelling and operation optimization of district heating systems. PhD thesis. Technical University of Denmark (DTU); 1991.

[16] Pálsson Halldór, Larsen Helge V, Bøhm Benny, Ravn Hans F, Zhou JiJun. Equivalent models of district heating systems for on-line minimization of operational costs of the complete district heating system, ISBN 87-7475-221-9. Number 1323.

[17] Bøhm Benny, Kristjansson Halldor. Single, twin and triple buried heating pipes: on potential savings in heat losses and costs. Int J Energy Res Nov 2005;29(14):1301–12. http://dx.doi.org/10.1002/er. 1118. ISSN 0363-907X, http://doi.wiley.com/10.1002/er.1118.

[18] Dalla Rosa A, Li H, Svendsen S. Method for optimal design of pipes for low-energy district heating, with focus on heat losses. Energy 2011;36(5):2407–18. http://dx.doi.org/10.1016/j.energy.2011.01.024. ISSN 03605442.

[19] Bøhm Benny. On transient heat losses from buried district heating pipes. Int J Energy Res 2000;24(15):1311–34. http://dx.doi.org/10.1002/1099-114X(200012)24:15¡1311::AID-ER648¿3.0.CO;2-Q. ISSN 0363-907X.

[20] Gabrielaitiene Irina, Bøhm Benny, Sunden Bengt. Modelling temperature dynamics of a district heating system in Naestved, Denmark-A case study. Energy Convers Manag 2007;48(1):78–86. http://dx.doi.org/10.1016/j.enconman.2006.05.011. ISSN 01968904.

[21] Irina Gabrielaitiene. Numerical simulation of a district heating system with emphases on transient temperature behaviour. In Environmental Engineering - The 8th International Conference, pages 747–754, Vilnius, Lithuania, 2011. ISBN 9789955288282.

[22] Stefan Grosswindhager, Andreas Voigt, and Martin Kozek. Linear Finite-Difference Schemes for Energy Transport in District Heating Networks. Proceeding of the 2nd International Conference on Computer Modelling and Simulation, (September):5–7, 2011.

[23] Van den Bossche Gertjan. Lokale temperatuurverhoging versus tijdmodulatie in lage temperatuur warmtenetten. Master thesis. Belgium: KU Leuven; 2015 [in Dutch].

[24] Jie Pengfei, Tian Zhe, Yuan Shanshan, Zhu Neng. Modeling the dynamic characteristics of a district heating network. Energy 2012;39(1):126–34. http://dx.doi.org/10.1016/j.energy.2012.01.055. ISSN 03605442.

[25] Dalla Rosa Alessandro, Li Hongwei, Svendsen Svend. Modeling transient heat transfer in small-size twin pipes for end-user connections to low-energy district heating networks. Heat Transf Eng 2013;34(4):372–84. http://dx.doi.org/10.1080/01457632.2013.717048. ISSN 0145-7632, http://www.tandfonline.com/doi/abs/10.1080/01457632.2013.717048.

[26] Fang Tingting, Lahdelma Risto. State estimation of district heating network

based on customer measurements. Appl Therm Eng Sep 2014;73(1):1209–19. http://dx.doi.org/10.1016/j.applthermaleng.2014.09.003. ISSN 13594311, http://linkinghub.elsevier.com/retrieve/pii/S1359431114007728.

[27] Oppelt Thomas, Urbaneck Thorsten, Gross Ulrich, Platzer Bernd. Dynamic thermo-hydraulic model of district cooling networks. Appl Therm Eng Jun 2016;102:336–45. http://dx.doi.org/10.1016/j.applthermaleng.2016.03.168. ISSN 13594311, http://linkinghub.elsevier.com/retrieve/pii/S1359431116304768.

[28] Modelica Association. Modelica – a unified object-oriented language for systems modeling language specification version 3.3 revision 1. 2014. https://www.modelica.org/documents/ModelicaSpec33Revision1.pdf.

[29] Dynasim AB. Dymola user's manual. Lund. 2004.

[30] Stéphane Velut and Hubertus Tummescheit. Implementation of a transmission line model for fast simulation of fluid flow dynamics. In Proceedings 8th Modelica Conference, pages 446–453, Dresden, 2011. URL http://www.ep.liu.se/ecp/063/049/ecp11063049.pdf.

[31] Loic Giraud, Roland Baviere, Mathieu Vallée, and Cédric Paulus. Presentation, Validation and Application of the DistrictHeating Modelica Library. In Proceedings 11th Modelica Conference, pages 79–88, Versailles, France, Sep 2015. doi: 10.3384/ecp1511879. URL http://www.ep.liu.se/ecp/_article/index.en.aspx?issue=118;article=8.

[32] Modelica Association. Modelica standard library. 2016. https://github.com/modelica/Modelica.

[33] Isoplus. Isoplus product catalog. 2016. http://www.isoplus.nl/.

[34] Frederiksen Svend, Werner Sven. District heating and cooling. first ed. Lund: Studentlitteratur AB; 2013.

[35] Benonysson Atli, Bøhm Benny, Ravn HF. Operational optimization in a district heating system. Energy Convers Manag 1995;36(5):297–314. http://www.sciencedirect.com/science/article/pii/019689049598895T.

[36] S. Mohammadi, C. Bojsen, and C. Milan. Identifying the optimal supply temperature in district heating networks - A modelling approach. In The 14th International Symposium on District Heating and Cooling, pages 1–6, Stockholm, 2014.

[37] Çengel Yunus A, Boles Michael A. Thermodynamics: an engineering approach. eight ed. New York, New York, USA: McGraw-Hill Education; 2014, ISBN 9789814595292.

[38] Kuosa Maunu, Kontu Kaisa, Mäkilä Tapio, Lampinen Markku, Lahdelma Risto. Static study of traditional and ring networks and the use of mass flow control in district heating applications. Appl Therm Eng May 2013;54(2):450–9. http://dx.doi.org/10.1016/j.applthermaleng.2013.02.018. ISSN 13594311, http://linkinghub.elsevier.com/retrieve/pii/S1359431113001233.

[39] Laajalehto Tatu, Kuosa Maunu, Mäkilä Tapio, Lampinen Markku, Lahdelma Risto. Energy efficiency improvements utilising mass flow control and a ring topology in a district heating network. Appl Therm Eng 2014;69(1–2):86–95. http://dx.doi.org/10.1016/j.applthermaleng.2014.04.041. ISSN 13594311, http://www.sciencedirect.com/science/article/pii/S1359431114003056.

[40] Michael Wetter, Marcus Fuchs, Pavel Grozman, Lieve Helsen, Filip Jorissen, Moritz Lauster, M Dirk, Christoph Nytsch-geusen, Damien Picard, Per Sahlin, and Matthis Thorade. IEA EBC Annex 60 Modelica library an international collaboration to develop a free open-source model library for buildings and community energy systems. In Proceedings of BS2015: 14th Conference of International Building Performance Simulation Association, pages 395–402, Hyderabad, India, 2015.